Supporting Information

Yun et al. 10.1073/pnas.1617666114

SI Text

Derivation of Natural Capital Asset Prices for Multiple Interacting Stocks. Let $s^i(t)$ be the i th natural capital stock of an N stock ecosystem, and let ds^i/dt describe the change in the capital stock i through time:

$$\frac{ds^i}{dt} = \dot{s}^i = G^i(\boldsymbol{s}(t)) - f^i(\boldsymbol{s}, \boldsymbol{x}(\boldsymbol{s}(t))),\ i = 1, \cdots, N, \qquad \textbf{[S1]}$$

where superscripts are indices;, $\boldsymbol{s}(t) = (s^1(t), s^2(t), \cdots, s^N(t))$ is a vector of multiple (natural) capital stocks at time t, and G^i is a growth function for stock i, which can be a function of other natural capital stocks. For example, in a biological system, G includes prey–predator relationships. The function f^i is an anthropogenic impact function (e.g., harvesting behavior) on stock i. The vector $\boldsymbol{x}$ represents human feedback responses shaped by governing institutions. Specifically, define $M(\boldsymbol{s}, \boldsymbol{\Omega})$ as a time-autonomous economic program that accounts for the vector of capital stocks and a vector of parameters defining institutional arrangements, $\boldsymbol{\Omega}$ (19, 23), that maps into a vector-valued function $M : (\boldsymbol{s}(t), \boldsymbol{\Omega}) \to \boldsymbol{x}(\boldsymbol{s}(t); \boldsymbol{\Omega})$, where the length of $\boldsymbol{x}$ is L and is not necessarily equal to the length of $\boldsymbol{s}$. We suppress the parameter vector $\boldsymbol{\Omega}$ when doing so does not cause confusion. To clarify, in a fishery, f^i may be harvest of species i, whereas $\boldsymbol{x}$ may include decisions, such as time at sea and gear choices, that combine with stock s^i to lead to f^i.

Define $D(\boldsymbol{s}(t), \boldsymbol{x}(\boldsymbol{s}(t)))$ as an index of the net benefits or dividends flowing to society at time t. Suppressing the dependence on time, assume that $D(\boldsymbol{s}, \boldsymbol{x}(\boldsymbol{s}))$ is measured in stable monetary terms, so that discounting at a constant exponential rate is justified (49). At a time t, the present value of net benefits is

$$V(\boldsymbol{s}(t)) = \int_t^{\infty} e^{-\delta(\tau - t)} D(\boldsymbol{s}(\tau), \boldsymbol{x}(\boldsymbol{s}(\tau))) d\tau. \qquad \textbf{[S2]}$$

The term δ is the social discount rate (e.g., the US Office of Management and Budget rate of 3%) (50). Substituting $\boldsymbol{x}(\boldsymbol{s})$, it is possible to redefine D over the stock vector $\boldsymbol{s}$, so that $D^*(\boldsymbol{s}(\tau)) \equiv D(\boldsymbol{s}(\tau), \boldsymbol{x}(\boldsymbol{s}(\tau)))$, where the asterisk indicates the elimination of $\boldsymbol{x}$. We slightly abuse notation and assume that the partial derivative of D includes the feedback through the economic program: $D^*_{s^i} = D_{s^i}(\boldsymbol{s}(\tau), \boldsymbol{x}(\boldsymbol{s}(\tau))) = \partial D/\partial s^i + (\nabla_{\boldsymbol{x}} D)' d\boldsymbol{x}/ds^i$, where $\nabla_{\boldsymbol{x}} D$ is the gradient vector of D with respect to $\boldsymbol{x}$, $d\boldsymbol{x}/ds^i$ is the $(L \times 1)$ derivative vector of $\boldsymbol{x}$ with respect to s^i, and $'$ indicates transpose. A similar substitution of the economic program into f^i yields $f^i(s, x(s)) = f^{i*}(s)$, so that $f^i_{s^i} = \partial f^i/\partial s^i + (\nabla_{\boldsymbol{x}} f^i)' d\boldsymbol{x}/ds^i = f^{i*}_{s^i}$. To be clear, the first step is substituting in the economic program. Therefore, although the second term looks like it comes from a total derivative, it is in fact just an application of the chain rule.

Substitution of the economic program into D, the assumption of an infinite time horizon, and assuming that the resource dynamics (Eq. **S1**) and economic program are time-autonomous enable V to be expressed solely as a function of $\boldsymbol{s}(t)$. The shadow price of stock i at time t for a given economic program is

$$p^i(\boldsymbol{s}(t)) \equiv \frac{\partial V(\boldsymbol{s}(t))}{\partial s^i(t)}. \qquad \textbf{[S3]}$$

Note that p^i is a function of all stocks, $\boldsymbol{s}$, rather than a single stock. Each stock can impact D, the stock dynamics, and the feedback rules embodied in $\boldsymbol{x}$. The asset price of p^i includes cross-stock effects (Eq. **1**).

Following the works by Dasgupta and Maler (32) and Arrow et al. (44) and adopting the definition (Eq. **S3**), we differentiate $V(\boldsymbol{s}(t))$ with respect to t and express it as

$$\frac{dV}{dt} = \delta V - D(\boldsymbol{s}, \boldsymbol{x}(\boldsymbol{s})) = (\nabla_{\boldsymbol{s}} V)' \frac{d\boldsymbol{s}}{dt} = \boldsymbol{p}(\boldsymbol{s})' \frac{d\boldsymbol{s}}{dt}, \qquad \textbf{[S4]}$$

where $\nabla_{\boldsymbol{s}} V$ is a $(N \times 1)$ gradient vector, $d\boldsymbol{s}/dt$ is an $(N \times 1)$ Jacobian matrix, and $\boldsymbol{p} = (p^1(\boldsymbol{s}), p^2(\boldsymbol{s}), \cdots, p^N(\boldsymbol{s}))$ is an $(N \times 1)$ shadow price vector. Eq. **S4** states that the time rate of change of the present value of benefits is equal solely to the effect from changes in the natural capital stocks evaluated at appropriate prices (19) or $dIW/dt = \boldsymbol{p}'\dot{\boldsymbol{s}} = dV/dt$. Rearranging the terms in Eq. **S4**,

$$\delta V = D(\boldsymbol{s}, \boldsymbol{x}(\boldsymbol{s})) + \boldsymbol{p}(\boldsymbol{s})' \dot{\boldsymbol{s}} = H(\boldsymbol{s}, \boldsymbol{x}, \boldsymbol{p}) = H^*(\boldsymbol{s}, \boldsymbol{p}). \qquad \textbf{[S5]}$$

$H^*(\boldsymbol{s}, \boldsymbol{p})$ is the current value Hamiltonian as evaluated along the economic program $\boldsymbol{x}(\boldsymbol{s})$, and it is composed of the flow of current benefits, $D(\boldsymbol{s}, x(\boldsymbol{s}))$, and the value of increments to the stocks, $\boldsymbol{p}'\dot{\boldsymbol{s}}$.

Dividing by δ on both sides, Eq. **S5** yields

$$V(\boldsymbol{s}) = \delta^{-1}(D(\boldsymbol{s}, \boldsymbol{x}(\boldsymbol{s})) + \boldsymbol{p}(\boldsymbol{s})' \dot{\boldsymbol{s}}), \qquad \textbf{[S6]}$$

which Shapiro and Stiglitz (51) call the fundamental asset equation. Differentiating Eq. **S6** with respect to s^i,

$$p^i(\boldsymbol{s}) = \frac{D_{s^i}(\boldsymbol{s}, \boldsymbol{x}(\boldsymbol{s})) + \left(\frac{\partial p^i}{\partial s^i} \dot{s}^i + \sum_{j \neq i}^{N} \frac{\partial p^j}{\partial s^i} \dot{s}^j \right) + \sum_{j \neq i}^{N} p^j \frac{\partial \dot{s}^j}{\partial s^i}}{\delta - \left(G^i_{s^i}(\boldsymbol{s}) - f^i_{s^i}(\boldsymbol{s}, \boldsymbol{x}(\boldsymbol{s})) \right)}. \qquad \textbf{[S7]}$$

After creating the definitions $MD^i \equiv D_{s^i}$, $MG^i \equiv G^i_{s^i}$, and $MHI^i \equiv f^i_{s^i}$ to preserve consistency with ref. 18, Eq. **S7** is identical to Eq. **1**.

The cross-price term, $\partial p^j/\partial s^i$, determines whether two stocks are capital complements or substitutes. Assuming that increasing stock i raises the value of $V(\boldsymbol{s})$ (i.e., stock i is an asset), then stocks i and j are only complements if $V_{s^i s^j}(\boldsymbol{s}) = \partial p^i(\boldsymbol{s})/\partial s^j > 0$. That is, endowing the system with more of stock j makes stock i more valuable. The reverse would be true if the stocks were substitutes, because the idea that stock j is a substitute for i implies that it can replace stock i, thereby lowering stock i's marginal value. We explore the slope of the level sets of the shadow price of $p^i = V_{s^i}$ in stocks i and j by invoking the implicit function theorem: $ds^j/ds^i = -(V_{s^i s^i}/V_{s^i s^j})$, where $V_{s^i s^i} = \partial p^i/\partial s^i$ and $V_{s^i s^j} = \partial p^i/\partial s^j$. Assuming that $\partial p^i/\partial s^i < 0$, a result that Fig. 2 shows holds in our case study, then $\partial p^i(\boldsymbol{s})/\partial s^j > 0$ implies upward sloping contours in state space for the case of complements. The reverse is true for the case of substitutes. However, the value of $\partial p^i/\partial s^j$ must be recovered jointly with shadow prices, and the shadow prices themselves are not obvious ex ante.

Approximating Shadow Prices. We use a polynomial approximation approach following refs. 18, 52, and 53 to approximate solutions to Eqs. **S2** and **S3**. The function approximation uses a linear combination of a series of nonlinear basis functions evaluated at a finite number of points in state space (53). We use Chebyshev polynomials for the basis functions. Chebyshev polynomials are used, because they have desirable orthogonality properties that enable them to provide the lowest error approximations to unknown functions, while also offering multiple differentiability (54, 55).

First, we located the evaluation nodes by specifying M univariate evaluation points for each of the N state variables and then calculated D and $\dot{s}^i$ at all combinations of these points. The evaluation nodes were selected by finding the M roots of each unidimensional Chebyshev polynomial on the bounded approximation interval of each state variable. Node coordinates were then combined to locate a node in multidimensional space. We define φ^i as the $M \times (q^i + 1)$ univariate basis matrix of q^i th degree over bounded ranges for each state variable. We expand the univariate bases matrices to allow for approximation over the bounded $\mathbb{R}^N$ domain by finding the tensor product across dimensions to form an $M^N \times \prod_{i=1}^{N}(q^i+1)$ basis matrix: $\Phi(\boldsymbol{S}) = \varphi^N \otimes \varphi^{N-1} \otimes \cdots \otimes \varphi^1$, where $\boldsymbol{S}$ is the $M^N \times N$ matrix of evaluation points (i.e., all grid nodes of M evaluation points for all N state variables), and $\otimes$ is the Kronecker product.

Second, we let $V^k(\boldsymbol{S}) \approx \Phi^k(\boldsymbol{S})\boldsymbol{\beta}$, where $k = 1, \ldots, M^N$ indexes the M^N distinct capital stock vectors (i.e., individual evaluation points in an N-dimensional grid) formed by the tensor product basis, $\Phi^k(\boldsymbol{S})$ is the kth row of $\Phi(\boldsymbol{S})$, and $\boldsymbol{\beta}$ is a $\prod_{i=1}^{N}(q^i+1) \times 1$ vector of unknown approximation coefficients. Stacking these M^S vector equations, we obtain the matrix equation:

$$V(\boldsymbol{S}) = \begin{bmatrix} \mathrm{V}^1(\boldsymbol{S}) \\ \vdots \\ \mathrm{V}^k(\boldsymbol{S}) \\ \vdots \\ \mathrm{V}^{M^N}(\boldsymbol{S}) \end{bmatrix} \approx \begin{bmatrix} \Phi^1(\boldsymbol{S}) \\ \vdots \\ \Phi^k(\boldsymbol{S}) \\ \vdots \\ \Phi^{M^N}(\boldsymbol{S}) \end{bmatrix} \boldsymbol{\beta} = \Phi(\boldsymbol{S})\boldsymbol{\beta}. \qquad \textbf{[S8]}$$

Using Eq. **S5** and the fact that $\partial V/\partial s^i(\boldsymbol{S}) = p^i(\boldsymbol{S}) \approx (\partial\Phi(\boldsymbol{S})/\partial s^i)\boldsymbol{\beta}$, we obtain $\delta\Phi(\boldsymbol{S})\boldsymbol{\beta} \approx D(\boldsymbol{S}) + \sum_{i=1}^{S} diag(\dot{s}^i)(\partial\Phi(\boldsymbol{S})/\partial s^i)\boldsymbol{\beta}$. Now let $M^N > \prod_{i=1}^{N}(q^i+1)$, so that it is not possible to satisfy the equality exactly at all approximation points. If we minimize the sum of squared approximation errors, then the resulting solution for $\boldsymbol{\beta}$ is

$$\boldsymbol{\beta} = (\Psi(\boldsymbol{S})'\,\Psi(\boldsymbol{S}))^{-1}\Psi(\boldsymbol{S})'\,D(\boldsymbol{S}), \qquad \textbf{[S9]}$$

where $\Psi(\boldsymbol{S}) = \delta\Phi(\boldsymbol{S}) - \sum_{i=1}^{N} diag(\dot{s}^i)\partial\Phi(\boldsymbol{S})/\partial s^i$.

With solutions for $\boldsymbol{\beta}$ in hand, we now have the ability to calculate the shadow prices at any vector of capital stocks in the approximation domain $\boldsymbol{s}$ through evaluation of the partial derivative of the basis vector: $p^i(\boldsymbol{s}) \approx (\partial\Phi(\boldsymbol{s})/\partial s^i)\boldsymbol{\beta}$. We implement the approximation using the R package {*capn*}, which is available at environment.yale.edu/profile/eli-fenichel/software.

Baltic Sea Model Adaptation Details. We adopt Hutniczak's (40) ecological–economic model of the Baltic Sea fishery that contains multiple agent and species interactions and follow her description of institutional arrangements. In this model, changes in the ecosystem result from species growth, predation, and individual fishing vessels' behaviors under a set of regulatory rules. Regulators annually set species-specific TACs based on single-species stock assessments and target fishing mortalities. Harvest allocations are distributed among vessels in the form of individual nontransferable quotas. We assume that vessels in the fishing fleet seek to maximize current net revenue through harvest choices—subject to regulations, physical constraints, owned capital, production structure, individual technical efficiency, and available stock abundance.

The biological component of the model includes age-structured submodels for cod, herring, and sprat linked through predation as described in appendix A of ref. 40. The International Council for the Exploration of the Sea (ICES) provides annual stock assessments for major Baltic Sea species. The model parameters (tables A1, A3, A4, and A6 of ref. 40) are updated based on the Report of the Baltic Fisheries Assessment Working Group (56) and available in Tables S1–S3.

The largest and only conceptual change in the current biological model relative to ref. 40 is that we follow the Report of the Benchmark Workshop on Baltic Multispecies Assessment (57) approach, and we estimate weight of cod recruitment ($w_{a,t}$; $a = 2$) as a function of parental weight (w_{SSB}) in addition to weight of adult cod ($w_{a,t}$; $a \geq 3$) as a function of the amount of prey available, with a indicating age.

$$w_{a,t} = \psi_1 + \psi_2 \ln\left(w_{SSB,t-2}\right); a \in [2] \qquad \textbf{[S10a]}$$

$$w_{a,t} = w_{a-1,t-1}\left(\theta_{a-1} + \frac{\left(\sum_{i\in(z,h)}\sum_{a=1}^{8} y_{i,a,t}\right)^n}{\left(\sum_{i\in(z,h)}\sum_{a=1}^{8} y_{i,a,t}\right)^n + {K_{sh}}^n}\right); a \in [3,8]. \qquad \textbf{[S10b]}$$

The subscripts z and h indicate prey species (sprat and herring, respectively); furthermore, y is the biomass, K_{sh} is the half-saturation constant, n is a functional response constant, and Greek letters are estimated parameters. Eqs. **S10a** and **S10b** are jointly estimated by generalize methods of moments with robust SEs using cod weight based on 1991–2014 data (56). Estimated parameters are provided in Table S4, and details on constants can be found in the work by Hutniczak (40).

The commercial harvest model closely follows the work by Hutniczak (40). Vessels operate as decision-making units that seek to maximize net revenue constrained by quota allocations, stock levels, and vessel characteristics, including technical efficiency constraints, through adjusting fishing behavior. The input requirement, the amount of effort required to land the chosen species composition in units of days at sea, is estimated with one-way fixed effects to account for the heterogeneity in fleet input efficiency, and estimation results are given in Table S5. This method offers the advantage of enabling us to account for effects, such as costly targeting and joint production. Landing price data calculated in 2013 Euros (EUR) are provided in Table S6. Data come from the Polish Fisheries Monitoring Centre in Gdynia, the Polish Marine Institute in Gdynia, and the 2015 Annual Economic Report on the European Union (EU) Fishing Fleet (36).*

We forecast two target fishing mortality scenarios. First, we consider BAU, which models historical and current policy. The fishing mortality rates associated with this case are 0.30, 0.26, and 0.29 for cod, herring, and sprat, respectively. Second, we adopt the MMSY approach suggested by the ICES (57) and planned for implementation in 2017. The mortality rates for this case are 0.55, 0.3, and 0.3 for cod, herring and sprat, respectively (40).

Data Generation. To implement the shadow price approximation approach, we generate an $M^N \times (2N+1)$ matrix of simulated (pseudo)data. There are M^N evaluation nodes, N columns of stock levels (three in our case study), N columns of changes in stock with respect to time $\dot{s}^i$ (three in the case study), and a column of dividend flows, D. The $M^N \times (2N+1)$ matrix must span over all regions of the state space for which we wish to calculate shadow prices (i.e., all combinations of stocks for each species). In practice,

*These data are individual logbook data with confidentiality protections for the individual vessel owners. They may only be accessed in cooperation with the Polish Fisheries Monitoring Centre in Gdynia, a part of the Polish Fisheries Department under the Ministry of Maritime Economy and Inland Waterways.

such data are rarely available, because observational time series data from ecological–economic systems rarely sample very broadly through the state space. "Pseudodata" generated by models can fill this gap—while also ensuring that the resulting data are consistent with the underlying bioeconomic model of the system (37).

Before generating the pseudodata, we must establish the domain that those data fill. This domain must be defined sufficiently broadly, so that it fully captures the system dynamics originating from any stock level for which one wants to produce a shadow price. We established the steady-state stock vector by simulating from 2013 initial conditions. By year 50 (2063), the stocks of the three species are stable at [cod, herring, sprat] = [439, 1,163, 1,252] thousand metric tons under the BAU scenario and [cod, herring, sprat] = [364, 1,585, 1,864] thousand metric tons under the MMSY scenario. In addition to these steady-state vectors, we also considered the range of the transition path to the steady state from the observed 2013 stocks [cod, herring, sprat] = [175, 1,303, 1,753] thousand metric tons as well as the recent range of the stocks in defining the domain for generating pseudodata.

For herring, we set the lower bound at 60% of the BAU steady-state biomass (698 thousand metric tons) and the upper bound at 140% of the BAU steady-state biomass (1,628 thousand metric tons). For sprat, we set the lower bound at 60% of the BAU steady-state biomass (751 thousand metric tons) and the upper bound at 160% of the BAU steady-state biomass (2,128 thousand metric tons). A greater relative range was used for sprat because of the large initial stock size. These ranges do a good job of capturing the full future projected trajectory and a large fraction of the historical stock sizes. The 2013 stock of cod and the recent historical cod biomass have been substantially lower than the steady state. Therefore, we set the lower cod bound at 130 thousand metric tons and the upper cod bound at 800 thousand metric tons, which capture both the recent history and projection values. The lower and upper bounds of domains also safely cover the range of the MMSY scenario.

Having established the domain, we generate a 20th-order three-dimensional Chebyshev polynomial defined over the domain for each of the three species and use the combined roots of these polynomials to establish 8,000 points at which to simulate the model. At each of these 8,000 simulation nodes, we simulate profit, D, and growth rates, $\dot{s}^i$. We use fixed biomass at age shares based on 2008–2013 averages to map the full age-structured model into a biomass dynamic model (Table S7). For estimates requiring a two period lag (e.g., cod recruitment), we use the same biomass at $t-1$ and t.

The bioeconomic simulation model solves for net revenue maximizing fishing effort for all individual Polish fishing vessels active in 2012. Then, for D, we sum over the fleet at each simulation node. We scale these predictions using multipliers, assuming that the Polish fleet is representative of the other fleets fishing in the Baltic Sea, to translate these sample results on fishing behavior and economic returns to the entire Baltic Sea fleet. We use fixed shares based on 2012 TAC distribution between EU members: 0.30 for cod, 0.28 for herring, and 0.29 for sprat. Our shares approach is justified, because allocation among EU members is based on the principle of relative stability, which implies that each country receives a fixed share of each TAC (58), and similarity of the composition of EU fleets participating in the Baltic Sea harvest (36). The results for the Polish fleet indicate that TAC utilization can vary considerably with changing individual quotas and biomass levels. The underutilization of TAC occurring in our model is an expected response to varying harvest conditions that cause lack of profitability for some quota combinations. Annual ICES reports show that historical TAC utilization was ∼39–89% (2010–2015[†]) for cod, ∼35–109% (1989–2015) for herring, and ∼41–103% (1987–2015) for sprat between 2008 and 2012. Our simulation results suggest that the TAC utilizations from our simulation model fall within realistic ranges.

The 8,000 simulation nodes create a somewhat "bumpy" surface linking the status of the three species, the economic program $\boldsymbol{x}(\boldsymbol{s})$, and hence, simulated profit D and growth rate $\dot{s}^i$. These irregularities create numerical issues for shadow price approximation because of their tendency to produce locally unstable estimates of derivatives. This bumpiness occurs, because the simulation compresses the decisions of 411 representative vessels over a state space of 24 age categories for three species down to three dimensions. The discrete changes of vessel behavior across this large, but finite, number of vessels at critical stock thresholds create small but nontrivial discontinuities in overall effort predictions from the simulations. The bumpiness of the implied surface can be viewed as a surface with discrete jumps that lead to the Gibbs–Wilbraham phenomenon (59). The Gibbs–Wilbraham phenomenon is an overshoot in the convergence of a functional approximation (i.e., Gibbs oscillations) in the neighborhood of a discontinuity of the function being approximated (60). High-dimensional Chebyshev approximations can be particularly vulnerable to Gibbs oscillations when fitted to a discrete sample of nodes (59).

To avoid these numerical problems, we avoid approximating the shadow prices on the raw pseudodata, but instead, we fit smooth, locally well-fitting surfaces for D and $\dot{s}_i$ and use the predictions from these fitted surfaces for the approximation of shadow prices. To accomplish this smoothing, we use the linear spline local fitting method applied to the 8,000 simulation nodes. This method performs well and demands fewer parameters compared with other options. The bandwidths are selected using cross-validation for each D and $\dot{s}^i$ linear spline. Adopting the fitted splines, we smooth the simulated population dynamics of each species using a linear approximation $[s^i(t+1) \approx s^i(t) + \hat{\dot{s}}^i(t)]$ and predicted profit $[\hat{D}(t)]$, where carets indicate the function relationship based on the splines. The percentage root mean square errors of three $\dot{s}^i$ (cod, herring, and sprat) and D are 5.78, 1.63, 0.48, and 0.71%, respectively, for the BAU and 1.07, 1.62, 0.56, and 0.51%, respectively, for the MMSY. This smoothing process provides reasonable derivatives, while capturing the overwhelming majority of information contained in the pseudodata. We compare simulation results from the original model with the smoothed model based on the linear splines, which are repeated from Fig. 1 (Fig. S1). An alternative to our smoothing approach would be to use a denser set of simulation nodes for the shadow price approximation. This alternative would further smooth the surface, allowing the shadow price approximation to occur without additional intermediate steps. However, generating the pseudodata requires that each of the 411 vessels solve a constrained optimization problem at each time step. It currently takes 21.7 h to generate the 8,000 nodes using 40 processors (48 gigabytes of random access memory) on the high-performance Omega computing cluster at the Yale Center for Research Computing. Our approach of fitting a smoothed model on a smaller set of nodes provides a computationally efficient approach that likely will be necessary for ecosystem management models with dimensions beyond our three-species model.

[†]We report cod TAC utilization for a shorter time series because of incomplete reporting and a considerable lack of enforcement in earlier years.

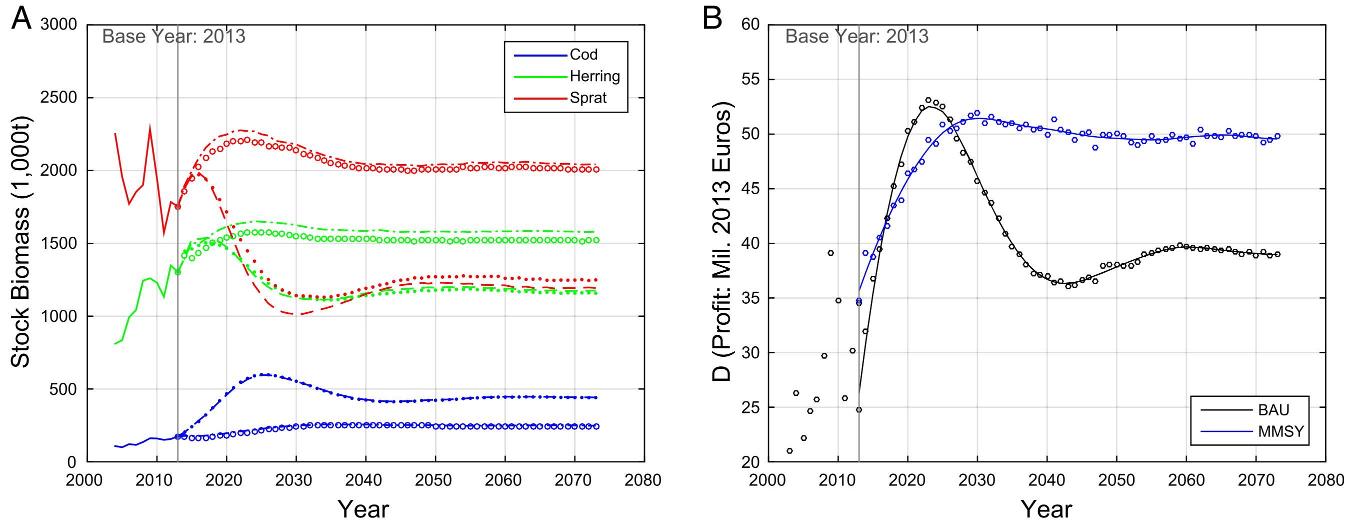

Fig. S1. The figure compares the original (circles) and smoothed (curves) simulations. *A* shows the ecological system, and *B* shows net revenue.

Table S1. Maturity rates and weights at age in stock (56). NA stands for not applicable

Age, y	1	2	3	4	5	6	7	≥8
Maturity, % of mature stock								
Cod	0.00	0.13	0.36	0.83	0.94	0.96	0.96	0.98
Sprat	0.17	0.93	1.00	1.00	1.00	1.00	1.00	1.00
Herring	0.00	0.70	0.90	1.00	1.00	1.00	1.00	1.00
Average weight 2008–2013, g								
Cod	NA	179	366	827	997	1,279	1,898	2,216
Sprat	5	9	10	11	11	11	12	12
Herring	13	22	28	32	37	41	46	51

NA, not applicable.

Table S2. Recruitment function coefficients (SEs) based on 1974–2014 data

Species	α_i: Intrinsic growth rate	β_i: Density dependence	γ_i: Environmental impact
Cod	0.382*** (0.086)	-1.32×10^{-3}*** (2.78×10^{-4})	0.304*** (0.052)
Sprat	4.745* (0.253)	-4.22×10^{-4}*** (2.35×10^{-4})	NA
Herring	3.574*** (0.134)	-6.74×10^{-4}*** (1.32×10^{-4})	NA

Cod recruitment dependent on environmental conditions is described by the average deep water salinity (*10% of significance level; ***1% of significance level). The source data are from ref. 56. NA, not applicable.

Table S3. Harvest parameters estimated from data from ref. 56 for years 2008–2013

Age, y	1	2	3	4	5	6	7	≥8
Selectivity—cod	NA	0.072 (0.014)	0.325 (0.031)	0.297 (0.028)	0.355 (0.024)	0.331 (0.051)	0.280 (0.064)	0.270* (0.085)
Selectivity—sprat	0.085 (0.009)	0.170 (0.012)	0.209 (0.016)	0.231 (0.012)	0.247 (0.011)	0.261 (0.017)	0.221 (0.025)	0.227 (0.027)
Selectivity—herring	0.026 (0.004)	0.056 (0.006)	0.093 (0.007)	0.119 (0.011)	0.130 (0.011)	0.150 (0.017)	0.189 (0.018)	0.174 (0.015)
Discard multiplier—cod	NA	2.038 (0.190)	1.314 (0.057)	1.152 (0.021)	1.122 (0.026)	1.059 (0.027)	1.028 (0.022)	1.014 (0.016)

SEs are in parentheses. All estimates are significant at the 99% confidence level, except those indicated (*significant at the 95% confidence level). NA, not applicable.

Table S4. Cod growth function coefficients estimated from the 2008–2013 data from ref. 56

Coefficient	ψ_1	ψ_2	ϑ_2	ϑ_3	ϑ_{4+}
Value	0.215***	0.119***	1.464***	1.717***	0.803***
SEs	−0.002	−0.009	−0.022	−0.013	−0.006

***At 1% of significance level.

Table S5. Input requirement coefficients

Coefficient	Vessels ≥12 m		Vessels 8–11.99 m	
α_c	0.162 (0.026)	***	0.311 (0.029)	***
α_h	0.164 (0.033)	***	0.017 (0.029)	
α_s	0.154 (0.034)	***	NA	
α_o	0.109 (0.025)	***	0.115 (0.029)	***
α_k	−1.031 (0.464)	**	−0.098 (0.211)	
α_{cc}	0.042 (0.007)	***	0.058 (0.007)	***
α_{ch}	−0.004 (0.002)	*	−0.012 (0.003)	***
α_{cs}	−0.006 (0.003)	**	NA	
α_{co}	−0.010 (0.002)	***	−0.041 (0.004)	***
α_{hh}	0.046 (0.008)	***	−0.001 (0.008)	
α_{hs}	−0.011 (0.003)	***	NA	
α_{ho}	−0.009 (0.003)	***	−0.020 (0.003)	
α_{ss}	0.051 (0.009)	***	NA	
α_{so}	−0.011 (0.003)	***	NA	
α_{oo}	0.026 (0.006)	***	0.042 (0.006)	***
α_{kk}	0.651 (0.934)		−0.049 (0.428)	
α_{kc}	−0.074 (0.017)	***	−0.018 (0.015)	
α_{kh}	−0.048 (0.028)	*	0.028(0.016)	*
α_{ks}	0.014 (0.023)		NA	
α_{ko}	−0.021 (0.025)		−0.025 (0.017)	
Fixed effects				
Individual	Yes		Yes	
Time	No		No	

NA, not applicable.
*At 10% of significance level.
**At 5% of significance level.
***At 1% of significance level.

Table S6. Summary of the landing price data in 2013 Euros per 1 kg fresh weight

Vessel length, m	Cod	Herring	Sprat	Other
8–9.99	1.261	0.427	0.318	1.164
10–11.99	1.280	0.388	0.358	0.610
12–17.99	1.147	0.370	0.274	0.434
18–23.99	1.104	0.340	0.270	0.431
≥24	1.055	0.362	0.275	0.527

The source data are from ref. 36.

Table S7. Fixed biomass at age shares based on the 2008–2013 data from ref. 56

Age, y	1	2	3	4	5	6	7	≥8
Cod	Not included	0.158	0.234	0.311	0.166	0.074	0.034	0.023
Sprat	0.293	0.310	0.181	0.095	0.064	0.031	0.014	0.012
Herring	0.184	0.216	0.176	0.140	0.108	0.077	0.043	0.056